Catalysis Letters 66 (2000) 147–153

MgF_2 as a non-conventional catalytic support. Surface and structure characterization

Maria Wojciechowska [a,*], Bogdan Czajka [b], Mariusz Pietrowski [a] and Michał Zieliński [a]

[a] *Faculty of Chemistry, A. Mickiewicz University, ul. Grunwaldzka 6, 60-780 Poznań, Poland*
E-mail: emawoj@main.amu.edu.pl
[b] *Central Laboratory of the Batteries and Cells, 61-362 Poznań, Poland*

Received 2 December 1999; accepted 12 April 2000

The paper presents results of studies on the structure of MgF_2 support, performed using various experimental methods such as XRD, IR, temperature-programmed techniques and low-temperature nitrogen adsorption. MgF_2 is characterized by an XRD spectrum with over 40 patterns, which enabled us to follow the changes in crystallite size and internal tension caused by the thermal treatment. TPE-H_2O and TG allowed an estimation of the surface OH groups concentration as $\sim$3–4 nm^{-2}.

Keywords: magnesium fluoride, surface properties, XRD, FTIR, TPE-H_2O, TG

1. Introduction

Our previous studies have shown that magnesium fluoride is an interesting support for different catalytic materials. It was a good support for transition metal oxides such as MoO_3 [1], V_2O_5 [2], WO_3 [3] and binary systems like CuO and Cr_2O_3 [4,5] as well as for metallic catalysts like ruthenium ones [6,7]. In particular the recent reports on the application of MgF_2 as a support for Pd and Ru catalysts in hydrodechlorination [8] and hydrodesulfurization reactions [7] and for binary Cu–Mn oxide systems for NO_x reduction [9] indicate its great potential. In view of the above, in this study an attempt was made to characterize in detail the structure and surface properties of MgF_2.

MgF_2 shows good thermal stability and significant hardness. It is an insulator with a broad band gap. The lack of lattice oxygen enables a study of the interaction between the oxygen from the supported active phase and the support, as well as the transformations of surface complexes during pretreatment and the reaction.

In this paper a detailed study of the crystal structure of MgF_2 support is reported. Also the effect of thermal treatment on the crystallite size and internal tension was examined using an XRD method. Moreover, the porous structure of MgF_2 support and the hydroxyl groups occurring on its surface were characterized.

2. Experimental

2.1. Preparation of magnesium fluoride

Magnesium fluoride was obtained by adding small portions of $MgCO_3 \cdot 3H_2O$ to an aqueous solution of hydrofluoric acid until neutralisation, and acidifying it by introducing a few additional drops of the acid. The precipitate was then aged at room temperature for a couple of days under stirring, followed by calcination at temperatures 673–1173 K. After calcination, MgF_2 was ground to obtain 0.2–0.5 mm mesh size. The samples were hereafter denoted with the symbols MF-X, where X stands for the calcination temperature (i.e., MF-4 for calcination at 673 K ($400 + 273$ K)).

2.2. XRD experiments

X-ray diffraction studies were performed with a Philips PW1050 instrument equipped with a Cu Kα source and Ni filter in the range of 3°–152° 2θ. Based on the (110), (220) and (330) reflections using Hall's method [10], the crystallite size and second type internal tension were measured. The reflections were indexed and the interplanar distances d were found using a Philips software ADP (automatic powder diffraction).

2.3. Surface area and pore volume measurements

The low-temperature adsorption of nitrogen was performed with an ASAP 2010 Micromeritics instrument. Specific surface area was determined using the BET method and pore size distribution was established on the basis of the BJH method, using a desorption isotherm. For the samples with the specific surface area below 3 $m^2\,g^{-1}$, it was determined from the low-temperature isotherm of krypton adsorption.

2.4. Mechanical resistance

The MgF_2 samples of the grain size 0.2–0.5 mm, annealed (calcined) at different temperatures were ground in a ball grinder for 2 h. After that the mean size of the

---

[*] To whom correspondence should be addressed.

grains was determined by using a granulometer Mastersizer S, made by Malvern. The suspensions of the materials used for granulometric studies were obtained by shaking the samples in a dilute solution of water glass (1 volume of water glass + 2 volumes of H_2O).

2.5. Infrared spectra

IR experiments were performed with a Bruker instrument model Vector 22. The spectra were recorded in the range 4000–1200 cm^{-1}. MgF_2 wafers ($\sim$4 $mg\,cm^{-2}$) were placed in a quartz cell equipped with NaCl windows. The samples were evacuated to reach the vacuum of the order of 10^{-4} Pa.

2.6. Temperature-programmed water elimination – TPE-H_2O

TPE-H_2O measurements were carried out with an ASAP 2010 Micromeritics instrument equipped with a conductivity detector. 99.995% purity argon was used as a carrier gas. 0.1 g of the sample was activated in a quartz U-shaped tube for 1 h at temperatures 373–873 K under argon flow. The measurements were performed after cooling the sample to 323 K under the Ar flow (30 $cm^3\,min^{-1}$), at a rate 10 $K\,min^{-1}$.

2.7. Thermogravimetric measurements

The measurements were performed at temperatures 303–1253 K using a differential thermoanalyser Netzsch STA C 3F, equipped with a TG measurement unit. The experiments were performed under nitrogen flow (99.995% purity) and temperature increase rates 8 $K\,min^{-1}$ for the sample of 0.3 g.

2.8. Surface concentration of OH groups

The concentration of surface OH groups (N_{OH}) was calculated on the basis of the amount of water desorbed in the temperature range 673–973 K (TPE-H_2O and TG results) using the formula [11]

$$N_{OH} = \frac{W_{OH} \times 10^{-2} \times N}{S_{N_2} \times 10^{18} \times M/2}\ (\mathrm{nm}^{-2}),$$

where N is Avogadro's number, M the molecular weight of the water, W_{OH} the amount of water (wt%) (columns 3 and 4 in table 5), S_{N_2} the specific surface area from N_2 adsorption in $m^2\,g^{-1}$.

3. Results and discussion

3.1. X-ray study

It is known that magnesium fluoride crystallises in the rutile type structure. The coordination surrounding of magnesium ions has a distorted octahedral shape, where the Mg–F distances are 1.94 Å for four fluorine ions and 1.99 Å for the other two [12].

Figure 1 presents the XRD spectrum of magnesium fluoride calcined at 1173 K (MF-9). It consists of over 40 diffraction patterns in the range of 2°–152° 2θ. No signals assigned to $MgCO_3$ (a precursor of MgF_2), MgO or other contaminants were detected.

The experimentally and theoretically determined interplanar distances as well as relative intensities of particular

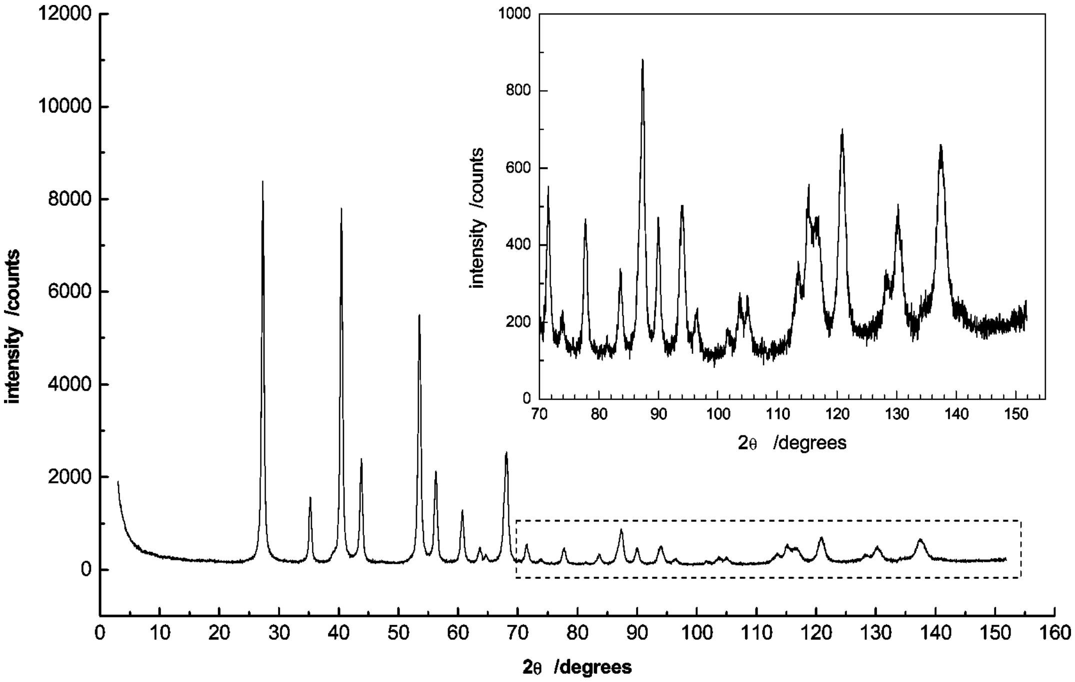

Figure 1. XRD spectra of MgF_2 calcined at 673 K.

Table 1
XRD characteristic of polycrystalline MgF_2.

No.	2θ	d_{exp}[a] (Å)	d_{calc}[b] (Å)	I/I_0[c]	hkl	No.	2θ (Å)	d_{exp}[a] (Å)	d_{calc}[b]	I/I_0[c]	hkl
1	27.34	3.2622	3.2647	100.0	110[d]	23	94.27	1.0518	1.0511	6.5	411
2	35.27	2.5447	2.5443	16.6	101	24	96.55	1.0329	1.0324	2.3	420
3	39.06	2.3062	2.3085	1.4	200	25	97.49	1.0255	1.0249	0.2	331
4	40.47	2.2287	2.2284	84.5	111	26	101.74	0.9938	0.9926	1.2	103
5	43.85	2.0645	2.0648	28.7	210	27	103.53	0.9815	0.9805	0.7	322
6	53.58	1.7104	1.7079	70.5	211	28	103.97	0.9785	0.9779	2.5	421
7	56.35	1.6327	1.6323	27.0	220[d]	29	105.01	0.9717	0.9704	2.7	113
8	60.68	1.5262	1.5390	16.4	300	30	113.08	0.9241	0.9234	0.7	500
9	63.71	1.4607	1.4643	4.1	310	31	113.64	0.9211	0.9202	4.3	402
10	64.74	1.4399	1.4391	2.1	221	32	115.19	0.9131	0.9119	9.3	213
11	67.76	1.3829	1.3814	11.4	112	33	116.58	0.9062	0.9055	4.4	510
12	68.22	1.3747	1.3739	32.9	301	34	117.16	0.9034	0.9025	5.4	412
13	71.66	1.3169	1.3168	5.9	311	35	120.79	0.8867	0.8857	7.7	332
14	74.05	1.2803	1.2805	1.3	320	36	121.29	0.8845	0.8838	8.7	431
15	74.82	1.2690	1.2722	0.6	202	37	126.35	0.8639	0.8628	0.5	223
16	77.84	1.2272	1.2265	5.6	212	38	127.47	0.8597	0.8573	1.8	520
17	81.50	1.1810	1.1806	0.6	321	39	128.56	0.8557	0.8548	4.2	422
18	83.80	1.1544	1.1542	3.6	400	40	130.39	0.8493	0.8481	10.8	303
19	86.98	1.1202	1.1198	4.1	410	41	134.72	0.8353	0.8342	1.8	313
20	87.48	1.1150	1.1142	12.4	222	42	137.88	0.8261	0.8253	21.4	521
21	90.17	1.0886	1.0882	6.2	330[d]	43	141.41	0.8168	0.8162	1.5	440[d]
22	93.85	1.0554	1.0545	3.4	312	44	150.66	0.7969	0.7961	0.3	323

[a] d_{exp} – experimental interplanar distances.
[b] d_{calc} – calculated interplanar distances.
[c] I/I_0 – relative intensity.
[d] Reflections used for the calculations of the crystallite size and the second type internal tension (summarized in table 2).

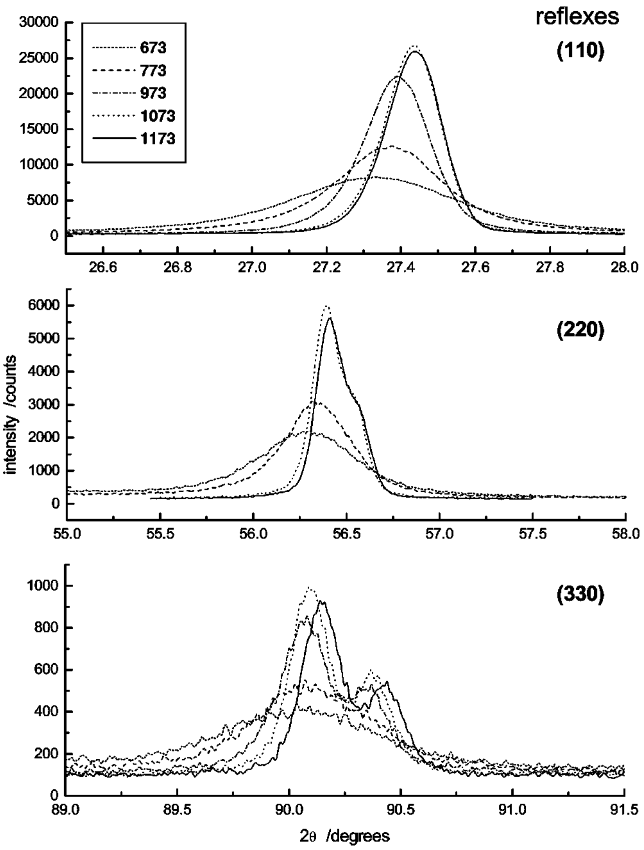

Figure 2. The effect of calcination temperature on the shape of XRD peaks of the (110), (220) and (330) planes of MgF_2.

Table 2
The effect of calcination temperature on the characteristics of MgF_2.

Calcination Temperature (K)	Calcination Time (h)	Average crystallite size (Å)	Internal tension (a.u.)	Mechanical resistance (a.u.)
673	4	216	11.4×10^{-4}	116
673	4[a]	215	11.0×10^{-4}	–
773	2	444	6.80×10^{-4}	146
973	2	1431	4.39×10^{-4}	195
1073	2	5260	2.80×10^{-4}	262
1173	2	9804	1.30×10^{-4}	347

[a] Sample was cooled in liquid nitrogen.

reflections are given in table 1. It is worth noting that the experimentally obtained data are very close to those obtained by theoretical calculations (the maximum difference is 0.0032 for the reflex No. 15). The calculated parameters for the elementary cell are as follows: $a = 4.6169$ Å, $c = 3.0492$ Å. The data presented in table 1 are more detailed when compared to those in ASTM card No. 6-0290 (1955) [13] which have been the best diffraction characteristics of polycrystalline MgF_2 available so far.

The presence of the three orders of reflections in the XRD spectra of MgF_2 gives an opportunity for studying the effect of the preparation parameters (such as calcination temperature, calcination atmosphere and cooling procedure) on the mosaic structure of magnesium fluoride. On the basis of the reflections from the planes (110), (220) and (330) (figure 2), the size of the crystallites and internal tension on the second type were calculated (table 2) using Hall's

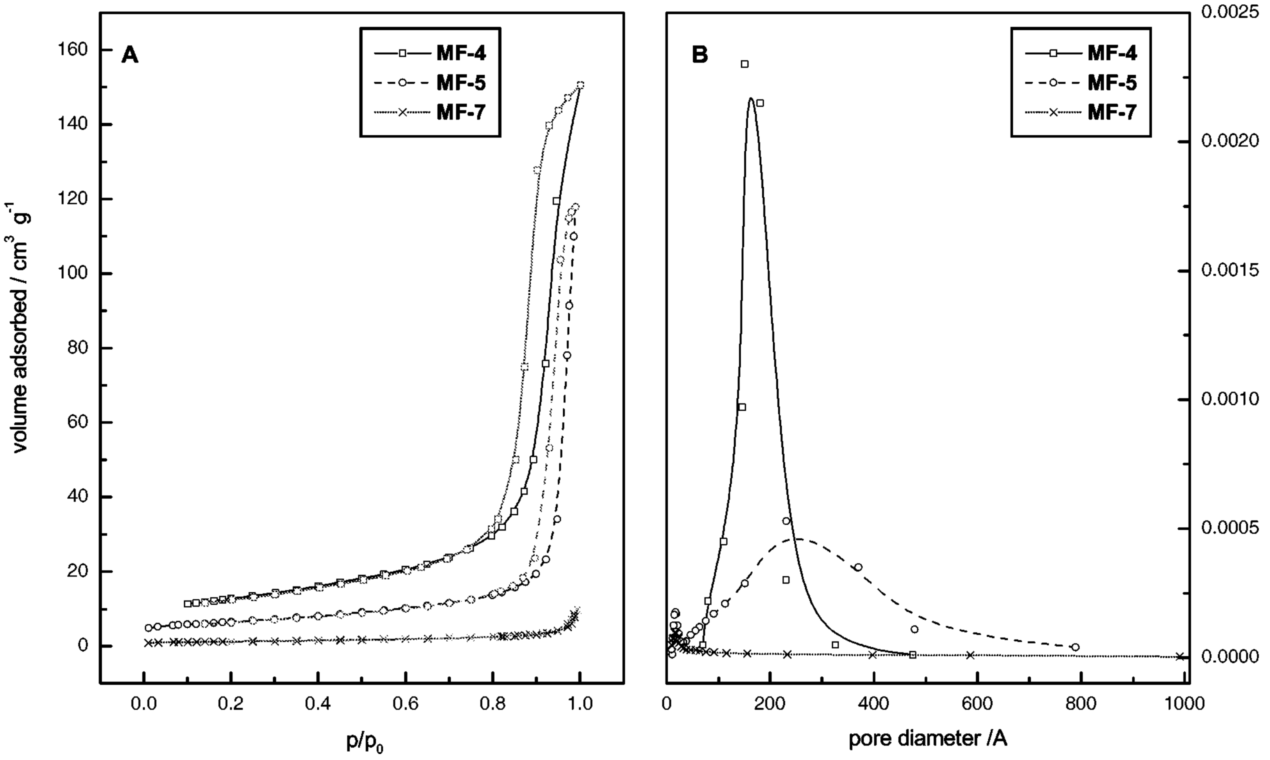

Figure 3. The effect of calcination temperature of MgF_2 on the nitrogen adsorption–desorption isotherms shape (A) and pore distribution (B).

method. Internal tensions of the second type determined by the "history" of the polycrystal, refer to the dislocations and defects in the area comparable with monocrystals. In such crystals the aggregates of non-ordered blocks with almost ideal internal structure are present. Since such a structure resembles a mosaic, it is called a mosaic structure. The effect of calcination temperature on the internal tension of the second type was found to be minor – one order of magnitude at the most, which indicates a well ordered mosaic structure (table 2). Similarly, the freezing of the sample structure by its sudden cooling from 673 K to the liquid-nitrogen temperature did not cause any tension. The values of internal strain for the MgF_2 cooled and not-cooled were very close (11.0×10^{-4} and 11.4×10^{-4}, respectively). On the other hand, the calcination conditions affected significantly the crystallite size, which varied from 216 to 9804 Å for the samples calcined at 673 and 1173 K, respectively. Similarly, the mechanical resistance of magnesium fluoride samples improved with the increase of the calcination temperature (table 2).

Detailed characteristics of the complex XRD spectrum enables us to follow the changes in MgF_2 structure during preparation and after introduction of the active phase using a sol–gel method. The latter is very important in respect to the observation of the support–active phase interaction.

3.2. Surface area and pore volume of MgF_2

Figure 3(A) presents the adsorption isotherms of MgF_2 samples calcined at 673, 773 and 1073 K. According to the IUPAC classification [14], they are type IV isotherms and the hysteresis loop are H1 type. Figure 3(B) shows the pore volume distribution as a function of pore diameter. The MF-4 sample is characterized by the pore size changing within a narrow range, with a maximum diameter of 160 Å. With increasing calcination temperature, the medium pore diameter increases, while the pore volume decreases. The H1 type of hysteresis loop indicates the narrow necks of the pores.

Table 3
Basic data of samples MgF_2 calcined at various temperatures.

Sample	Calcination temperature (K)	Surface area ($m^2 g^{-1}$)	Total pore volume ($cm^3 g^{-1}$)	Average pore radius (Å)
MF-4	673	44.6	0.228	164
MF-5	773	22.7	0.182	291
MF-6	873	18.8	–	–
MF-7	973	4.3	0.014	190
MF-8	1073	0.51	–	–

The data in table 3 illustrate the effect of calcination temperature on the surface area, medium pore radius and pore volume. Magnesium fluoride calcined at 673 K has a specific surface area of the order of 44.6 $m^2 g^{-1}$, however, calcination at higher temperatures resulted in a decrease of the surface area. The MgF_2 preparations obtained by thermal treatment in temperatures not higher than 873 K, show the surface texture which enables their use as catalytic support. Above 873 K the sintering of fine pores became significant and the specific surface area drastically decreased.

The results obtained indicate that MgF_2 calcined at 673 K is characterized by pore size varying in a narrow

Table 4
Characteristics of hydroxyl groups present on the surface of MgF_2 and their IR frequencies [1].

Type of OH group	CN of the surface cation	Net electric charge of OH group	OH groups IR wavenumbers
I[a]	VI	−0.7	3750, 3614, 3400
II[b]	V and V	−0.2	3750, 3614, 3400
III[c]	V	−0.6	3750, 3614, 3400

[a] OH group situated directly over an Mg^{2+} ion with CN = 5.
[b] OH group located between two Mg^{2+} ions with CN = 4.
[c] OH group situated over an Mg^{2+} ion with CN = 4; the Mg–OH bond is perpendicular to the latice plane.

range in the mesoporous region. Thus it can be used as a model mesoporous support.

3.3. IR results

According to the surface structure of MgF_2 [1,15] it includes the coordinatively unsaturated Mg^{2+} ions with the coordination number (CN) 4 and 5 (planes (110) and (001)) and also coordinatively unsaturated fluorine ions (in the (001) plane). During preparation or contact with water vapours, water dipoles interact with coordinatively unsaturated cations filling their coordination sphere and forming surface hydroxyl groups. The types and charges (calculated on the basis of a simple ionic model) of different surface hydroxyl groups of MgF_2 are presented in table 4. The negative charge of the OH groups testifies to their basic nature. All these groups give absorption bands in IR region 3800–3200 cm^{-1}.

Figure 4 presents the IR spectra of MF-4 treated in vacuum at different temperatures. In the spectrum of the sample evacuated for 30 min at room temperature a series of bands originated from hydroxyl groups can be observed. The increase of the evacuation temperature resulted in a decrease of the bands intensity or even in their complete disappearance. After evacuation at 673 K only three bands were recorded at ∼3750, 3614 and 3400 cm^{-1}. The two former bands originated from the vibrations of isolated OH groups, while the latter was attributed to OH groups bonded via the hydrogen bridge. The further increase of the evacuation temperature resulted in a gradual decrease of the intensity of those bands. The evacuation at 873 K resulted in a complete disappearance of the band at 3400 cm^{-1}. The IR spectra presented show also the bands characteristics of water molecularly adsorbed on magnesium ions at 1639 and 1669 cm^{-1}. The intensities of these bands, similarly as those assigned to OH groups, gradually decreased with increasing evacuation temperature. As follows from the above results, the temperature of 873 K is sufficient for total dehydroxylation of the MgF_2 surface.

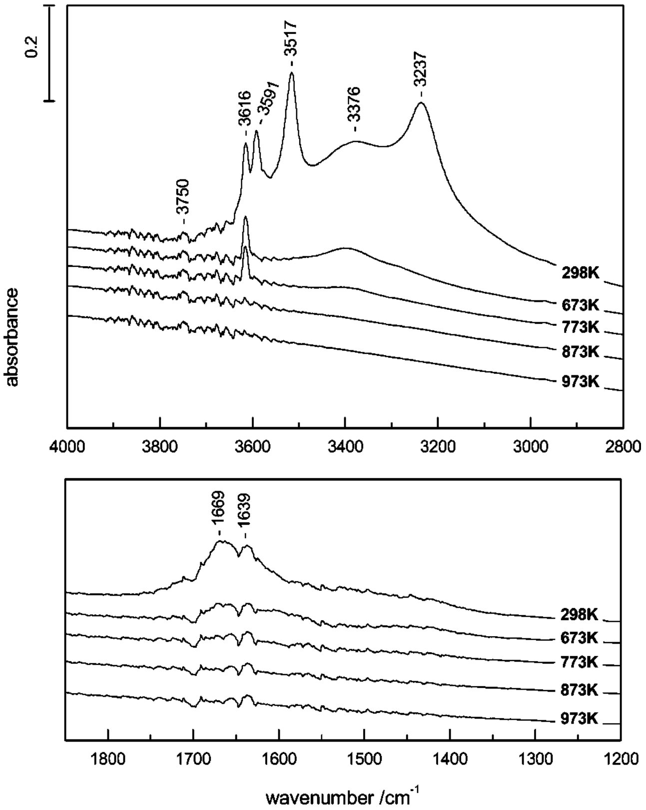

Figure 4. IR spectra of the MF-4 sample evacuated at different temperatures for 30 min.

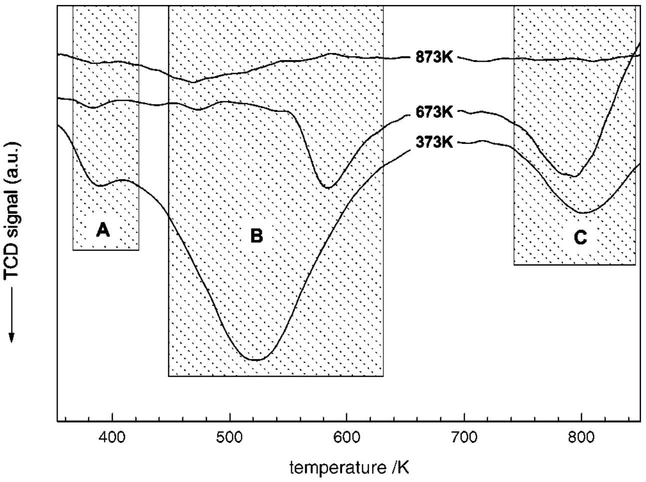

Figure 5. TPE-H_2O profiles of the MF-4 sample activated at different temperatures.

3.4. Teperature-programmed elimination of water ($TPE-H_2O$) and thermogravimetry (TG)

The hydroxyl groups occurring on the support surface are know to be of key importance in the process of the active phase introduction. In this study an attempt was made to estimate their concentration by using the TPE-H_2O and TG techniques.

In the TPE-H_2O spectra of MgF_2 (MF-4) activated for 1 h at 393 K three desorption peaks with maxima at ∼350 K (peak A), 500 (peak B) and 800 (peak C) were observed (figure 5). Peak B seems to be composed of a few superimposing peaks. The former originated from physically adsorbed water while the latter two from the molecularly

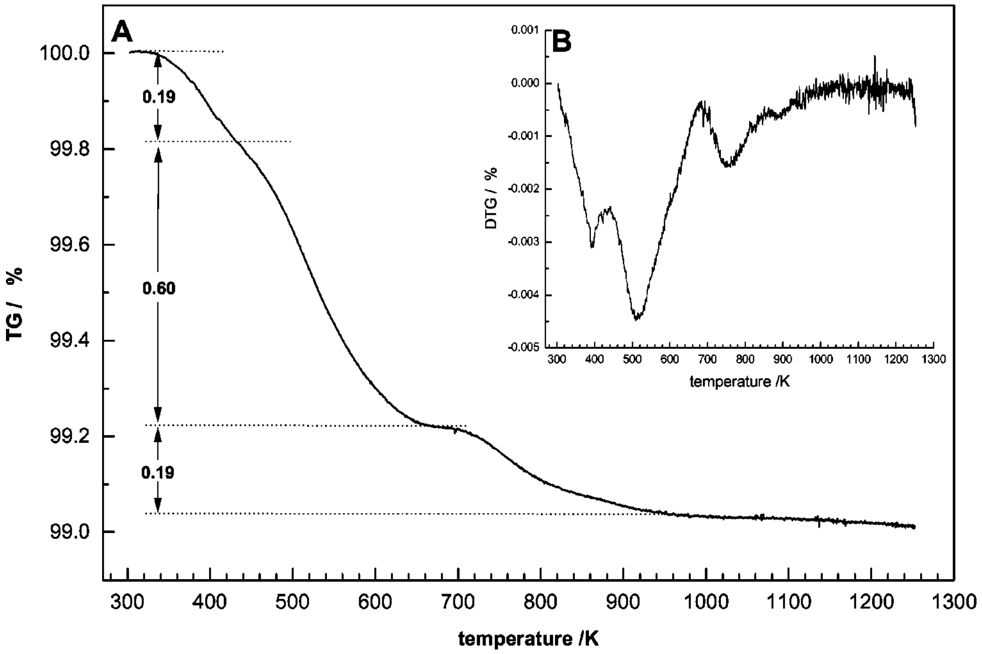

Figure 6. Thermogravimetric spectra of the the MF-4 sample: (A) TG curve and (B) DTG curve.

Table 5
Amount of different types of adsorbed water on MgF_2 surface.

H_2O	Desorption temperature (K)	H_2O (wt%)	
		TPE-H_2O	DTG
A (physisorbed)	298–433	0.05–0.07	0.19
B (chemisorbed)	433–673	0.82–1.18	0.60
C (dehydroxylated)	673–973	0.20–0.28	0.19

chemisorbed water and surface OH groups. The increase of the activation temperature resulted in a gradual disappearance of the low-temperature part of the spectrum. After the activation at 673–773 K, no peak assigned to physically adsorbed water (peak A) was observed, while the peak B became less intense. A 1 h activation at 873 K resulted in a complete removal of all types of adsorbed water and OH groups. These results are in agreement with those of IR experiments, where after activation of the sample at 873 K no bands originating from the vibrations of adsorbed OH groups or adsorbed water were recorded in the spectra.

Similarly to TPE-H_2O results, also thermogravimetric analysis revealed the presence of three peaks (figure 6). Thus it was concluded, that the only compound released during the thermal treatment was water.

On the basis of the TPE-H_2O and thermogravimetric studies, the number of water molecules involved at particular stages of elimination were established (table 5). In the sample treated at 673 K, which had the best properties from the catalytic point of view, the number of OH groups was in the order of 3–4 nm^{-2}. For the sake of comparison, for Al_2O_3 (673 K) this number is 5–6 OH groups per nm^2 [16]. Figure 7 shows a schematic location of OH groups on the (001) plane of the surface of MgF_2. The heterolytic dissociation of water occurs mainly in this plane, which results in hydroxylation of MgF_2 (observed by XPS and IR) [10].

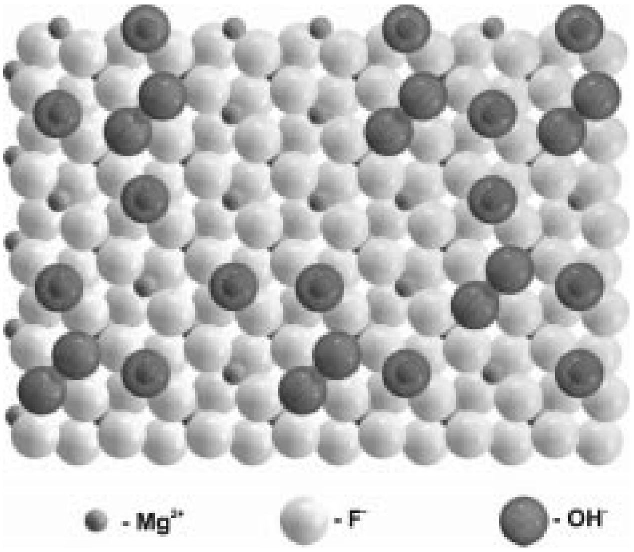

Figure 7. The arrangement of OH groups on the (001) crystal plane of MgF_2.

The surface model of MgF_2 is presented in [1]. In this paper the positions of surface hydroxyls, Mg–OH, and Mg–$(OH)_2$ were presented.

4. Conclusion

Detailed studies of magnesium fluoride crystalline structure, porosity and hydroxyl cover have been performed. XRD spectra of MgF_2 are very complex. The data reported in this paper provide the most comprehensive characteristics of polycrystalline MgF_2, more complete than in the ASTM card. The presence of the three sets of peaks in the XRD spectra of MgF_2 gives an opportunity for studying the effect of various preparation parameters of the catalysts on the mosaic structure of MgF_2. Moreover, the lack of oxygen atoms in the crystalline lattice of MgF_2 makes it possible to analyse the structure of oxide phases supported on magnesium fluoride.

Thermal treatment of MgF_2 in temperatures not exceeding 873 K, gives the preparations characterized by the surface area and porous structure, which make them suitable as active phase supports.

MgF_2 calcined at 673 K is characterized by the narrow pore size distribution in the mesoporous range, and thus it can be a model mesoporous support.

The characterization of hydroxyl groups occurring on the surface of MgF_2 was made. Three kinds of OH groups differing in basicity were distinguished and their concentration was for the first time estimated.

According to the results obtained, magnesium fluoride satisfies the criteria of a good catalytic support and can be successfully used in catalytic processes.

References

[1] J. Haber and M. Wojciechowska, J. Catal. 110 (1988) 23.
[2] J. Haber and M. Wojciechowska, Catal. Lett. 10 (1991) 271.
[3] M. Wojciechowska, W. Gut and V. Szymenderska, Catal. Lett. 7 (1990) 431.
[4] M. Wojciechowska, S. Łomnicki, J. Bartoszewicz and J. Goslar, J. Chem. Soc. Faraday Trans. 91 (1997) 2207.
[5] M. Wojciechowska, J. Haber and S. Łomnicki, J. Mol. Catal. 141 (1999) 155.
[6] M. Wojciechowska, M. Pietrowski, S. Łomnicki and B. Czajka, Catal. Lett. 46 (1997) 63.
[7] M. Wojciechowska, M. Pietrowski and S. Łomnicki, J. Chem. Soc. Chem. Commun. (1999) 463.
[8] A. Malinowski, W. Juszczyk, J. Pielaszek, M. Bonarowska, M. Wojciechowska and Z. Karpiński, J. Chem. Soc. Chem. Commun. (1999) 685.
[9] M. Wojciechowska, M. Zieliński and S. Łomnicki, in: *Proc. III Int. Conf. Catalysis and Adsorption in Fuel Precessing and Environmental Protection*, Kudowa, September 1999 (Oficyna Wydawnicza Politechniki Wrocławskiej, 1999) p. 249.
[10] A. Taylor, *X-Ray Metallography* (Wiley, New York, 1961) p. 778.
[11] B.G. Linsen, *Physical and Chemical Aspects of Adsorbents and Catalysts* (Academic Press, London, 1970) p. 258.
[12] A.F. Wells, *Structural Inorganic Chemistry*, 3rd Ed. (Clarendon Press, Oxford, 1962) p. 337.
[13] NBS Circular 539, Vol. IV (1955) 33.
[14] K.S.W. Sing, D.H. Everett, R.A.W. Haul, L. Moscou, R.A. Pierotti, J. Rouquérol and T. Siemieniewska, Pure Appl. Chem. 57 (1985) 603.
[15] M. Wojciechowska, Polish J. Appl. Chem. 40 (1996) 151.
[16] B.C. Gates, *Catalytic Chemistry* (Wiley, New York, 1992) p. 325.